AN EXPERIMENTAL INVESTIGATION OF THE TEMPERATURE FIELD PRODUCED BY A SURGICAL CRYOPROBE

William Kirk Petrovic

NAVAL POSTGRADUATE SCHOOL
Monterey, California

THESIS

AN EXPERIMENTAL INVESTIGATION
OF THE TEMPERATURE FIELD
PRODUCED BY A SURGICAL CRYOPROBE

by

William Kirk Petrovic

Thesis Advisor: Thomas E. Cooper

December 1972

Approved for public release; distribution unlimited.

An Experimental Investigation of the Temperature Field Produced by a Surgical Cryoprobe

by

William Kirk Petrovic
Lieutenant Commander, United States Navy
B.S. C. W. Post College, 1963

Submitted in partial fulfillment of the
requirements for the degree of

MASTER OF SCIENCE IN MECHANICAL ENGINEERING

from the

NAVAL POSTGRADUATE SCHOOL
December 1972

ABSTRACT

The temperature field produced by a cryosurgical probe embedded in a clear gelatin-water test medium has been experimentally investigated. The temperature field emanating from the cryoprobe was measured using a thin mylar sheet sprayed with liquid crystals, a temperature sensitive material. Probe tip temperatures varying from -36°C to -117°C were studied. The experimental results compared within approximately 9% of a one dimensional analytical solution for predicting ice growth rate.

TABLE OF CONTENTS

LIST OF FIGURES

NOMENCLATURE

c - specific heat in the unfrozen region cal/g/°C

c_f - specific heat in the frozen region cal/g/°C

k - thermal conductivity of the unfrozen region cal/sec/cm/°C

k_f - thermal conductivity of the frozen region cal/sec/cm/°C

L - latent heat of fusion cal/g

r - radial distance cm

r_o - radius of cryoprobe cm

$\mathcal{R}$ - radial location of the frozen/unfrozen interface cm

t - time sec

T - temperature in the unfrozen region °C

T_f - temperature in the frozen region °C

T_o - initial medium temperature °C

T_{pc} - phase change temperature °C

T_s - cryoprobe tip temperature °C

ρ - density g/cm^3

Nondimensional groups

$r^* = \mathcal{R}/r_o$

$R = r/r_o$

$\tau = -(1 + \phi)$ lesion growth constant

$$\theta = \frac{T - T_o}{T_s - T_o}$$

$$\theta_f = \frac{T_f - T_o}{T_s - T_o}$$

$$\theta_{pc} = \frac{T_{pc} - T_o}{T_s - T_o}$$

$$\theta^* = \frac{T_{pc} - T_s}{T_{pc} - T_o}$$

$$\phi = \frac{k_f}{k} \left(\frac{1 - \theta_{pc}}{\theta_{pc}}\right)$$

$$\tau = \frac{k \left(T_o - T_{pc}\right) t}{\rho L r_o^{\,2}}$$

ACKNOWLEDGEMENT

A deep sense of appreciation is expressed for the continued guidance and inspiration given to this researcher during the period of investigation by the thesis advisor, Professor Thomas Cooper. I also wish to thank Mr. George Baxter for his help in designing and constructing the two cryoprobes, Mr. Howard Bensch for his instruction in photographic technique, and Professor George Trezek for providing the CE-8.

Finally, I wish to express my appreciation to my wife, Nancy, who provided moral support during periods of frustration and who assisted in the preparation of the final draft.

I. INTRODUCTION

The use of low temperatures as a medical tool is not new. As early as 3500 B.C. the Egyptians used ice as a local anesthetic by applying it to wounds and other ailments. However, it was not until 1851 that extreme cold was used as a surgical procedure. Dr. James Arnott, a British physician, used a small container filled with an ice-brine mixture at -24°C as a surgical instrument. The container was placed in direct contact with skin cancers and was found helpful in restricting the growth of the cancerous tissue. In 1961, with the development of the first cryosurgical probe for the treatment of Parkinson's Disease, cryosurgery became an established surgical procedure. Dr. Irving Cooper of the Saint Barnabas Hospital in New York is acknowledged as the founder of the present day cryosurgical technique. Cooper developed a small multi-tubed probe with a hemispherical tip. The temperature of the tip could be controlled from body temperature, 37°C, to -196°C by circulating liquid nitrogen through it [4].

The cryoprobe has primary and secondary applications in treating diseases of the brain. The major use has been in the production of discrete destructive thalamic lesions in the surgical treatment of Parkinson's disease and related disorders. Unfortunately, the application of the cryosurgical technique to the management of benign or malignant tumors has been severely limited due to an inability to

predict lesion growth rate and ultimate lesion size [17]. There have been several analytical models developed for predicting lesion growth rate and size [1, 6, 7]. However, these models have yet to be verified experimentally.

The objectives of this thesis were: 1) to experimentally determine the growth rate of the frozen region around a cryoprobe 2) to investigate the feasibility of using liquid crystals, a material that indicates temperature through a change in color, as a temperature sensing device in the unfrozen region 3) to compare the experimentally determined temperatures and ice growth rates with existing analytical predictions.

Two cryoprobes, 0.5 inches and 0.187 inches in diameter, were designed and built along the lines of the standard Linde cryoprobe. The larger probe, which was intended as a prototype, produced ice regions that were approximately spherical in nature and easily studied. The smaller probe, due to faulty design, produced irregular regions that did not submit to detailed study. A 0.15% gelatin 99.85% water test medium was used to simulate tissue. A range of probe tip temperatures varying from -36°C to -117°C were used to create the frozen regions. In all cases studied, experimental and analytical predictions of ice growth rates compared within the estimated experimental uncertainty of 9%. The details of the magnitude and extent of the temperature field in the unfrozen region were successfully obtained with the liquid crystal material.

II. DESIGN OF THE SURGICAL CRYOPROBE

The general surgical cryoprobe used for necrotizing brain tumors consists of three concentric tubes [17]. The coolant, which is normally liquid nitrogen (LN_2), flows down the inner tube and absorbs heat from the tip, causing the coolant to vaporize. The vapor flows back through the middle annulus. The outer annulus is evacuated to minimize heat transfer between the gelatin and the returning vapor (Figure 1). Probe tip temperature is controlled by the coolant flow rate, which is in turn controlled by regulating the outlet pressure from the coolant supply reservoir.

The original desire was to determine the ice formation rate on an existing Linde cryosurgical unit. Attempts to secure such a unit were unsuccessful resulting in a need to construct a unit. Using the basic design of a Linde cryoprobe [17] as a model, two probes were designed and fabricated from stainless steel hypodermic tubing. The first cryoprobe built was a prototype. It was 0.5 inches in diameter and 5.75 inches in length (Figure 2, 3). The prototype was tested and found to work satisfactorily. The same design was applied to a smaller cryoprobe, 0.187 inches in diameter. This cryoprobe is the same size as the Linde Cryoprobe PR-2 used for brain tumors. When the smaller cryoprobe was tested, it failed to form a spherical ice ball. Instead, an elliptical ice ball formed indicating two problem areas. The vacuum volume was too small and the tip was not a

hemisphere but was shaped more like a cylinder. A new design should employ a smaller inner tube for the LN_2 to flow through and the tip should be a hemisphere as in the case of the large probe. The remainder of this thesis will be concerned with the 0.5 inch cryoprobe.

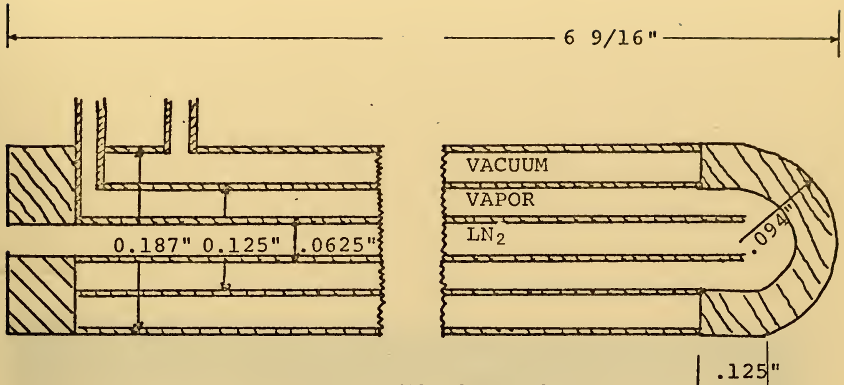

0.187 INCH CRYOPROBE

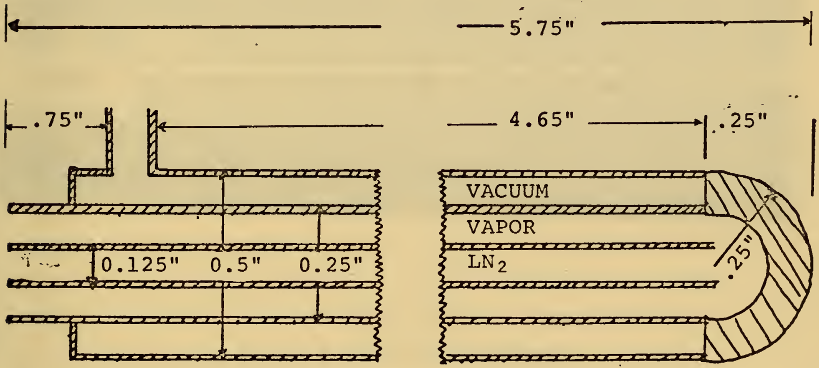

0.5 INCH CRYOPROBE

FIGURE 1

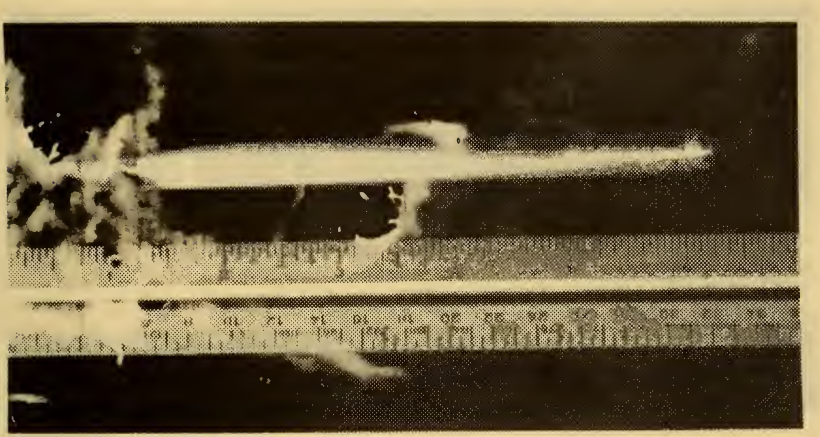

0.5 x 5.75 INCH CRYOPROBE

FIGURE 2

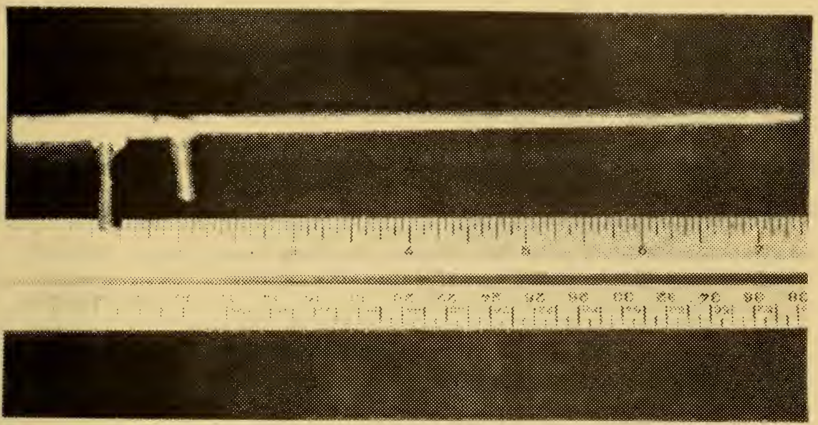

0.187 x 6.56 INCH CRYOPROBE

FIGURE 3

III. EXPERIMENTAL APPARATUS

The experimental set-up used in the present studies was similar to the set-up used by Groff in his studies of the resistively heated surgical probe [14]. Briefly, the set-up consisted of a 8 inch cubical test cell, with the cryoprobe horizontally inserted through a small hole in the center of one side of the test cell. The liquid crystal material, which was sprayed on a mylar sheet, was placed in the horizontal midplane of the cryoprobe. The probe had thermocouples welded on the tip and on the midpoint of the stem. The test cell was filled with a clear 0.15% gelatin /99.85% water test medium, which had the following thermal properties

a. k_f = .0050 cal/sec/cm/°C

b. k = .0014 cal/sec/cm/°C

c. L = 79.71 cal/g

The cryoprobe was connected to a LN_2 source. In order to record the visual data presented by the liquid crystals, a Graflex Camera was placed directly above the cryoprobe tip (Figure 4).

A. LIQUID NITROGEN SYSTEM

The LN_2 was stored in a Union Carbide CE-8, which is a dewar that uses the pressure of the vaporized LN_2 as the driving potential to force the LN_2 through a regulating valve. The unit is also equipped with a heater which can

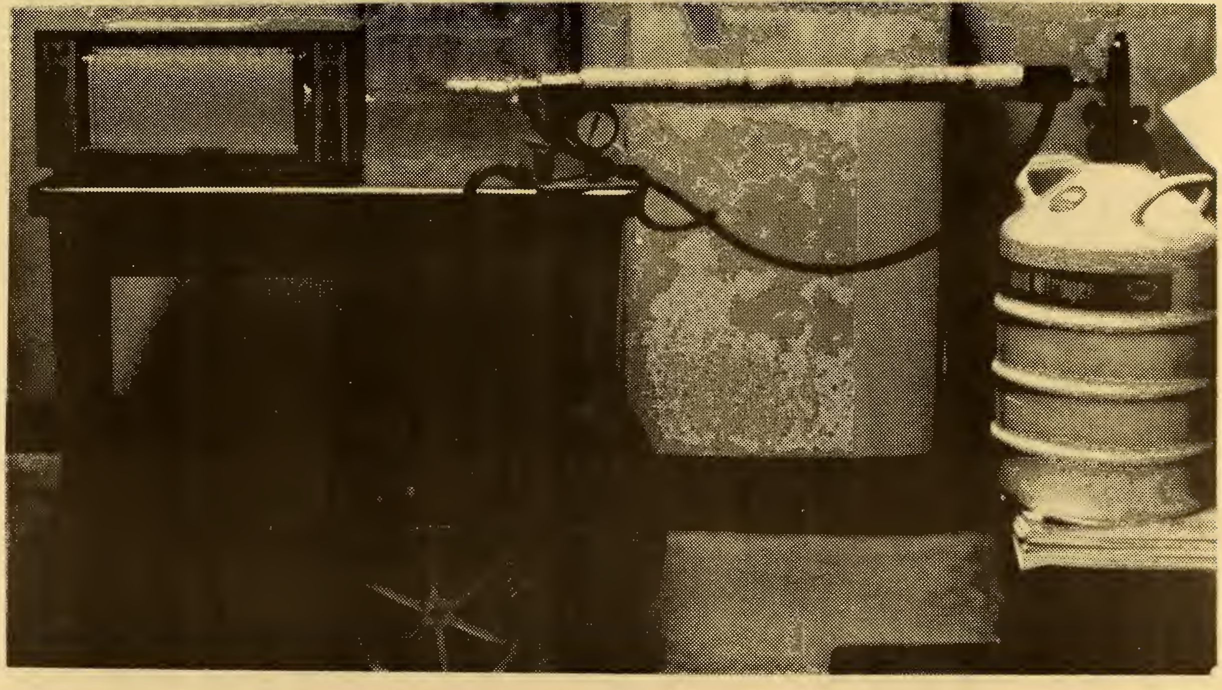

EXPERIMENTAL SET-UP

FIGURE 4

be used to vaporize the LN_2 to increase the pressure as necessary. The maximum working pressure of the system is 10.5 psig. The regulating valve is a needle valve that allows the operator to regulate the flow of the LN_2 (Figure 5).

To transfer the LN_2 from the dewar to the cryoprobe a connecting tube was designed and built (Figure 6). The tube is essentially two concentric tubes. The LN_2 flows through the inner annulus and the outer annulus is evacuated. The entire tube is encased in neoprene insulation.

B. LIQUID CRYSTALS

There are three types of liquid crystals; smectic, nematic and cholesteric [12, 13, 15, 16]. This experimental study used only the cholesteric type. A cholesteric liquid crystal responds to changes in temperature by sequentially passing through the complete visual spectrum (red through violet) in fractions or multi-degrees, depending on which cholesterol esters comprised the formulation. This color phenomenon is reversible. A very important point is that at a certain temperature a given material or combination of materials will always exhibit the same color. The light scattered by the liquid crystals represents only a fraction of the incident light. The remaining portion of the incident light is transmitted by the liquid crystals. Therefore, an absorptive black background must be used to prevent reflection of the transmitted light, thereby enhancing the color resolution.

LN_2 STORAGE UNIT CE-8

FIGURE 5

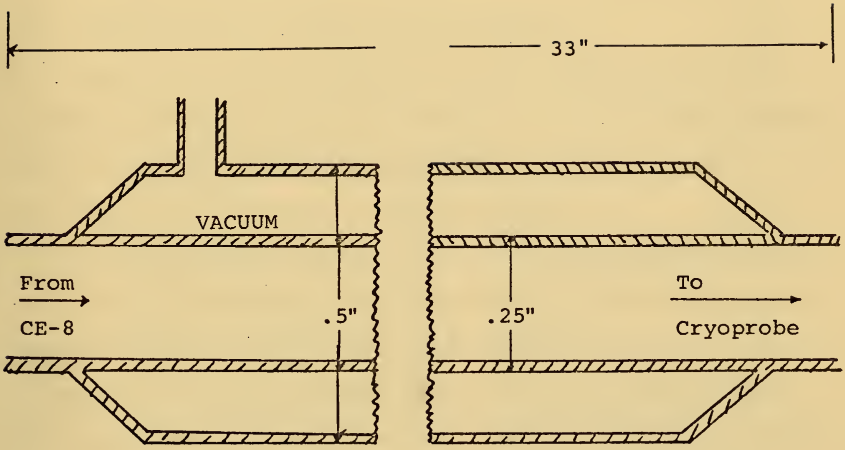

TRANSFER ANNULUS

FIGURE 6

Since the colors exhibited by the cholesteric liquid crystal are unique for a specific temperature, the quantitative measurement of temperature is possible to an accuracy of approximately 0.1°C, while the speed of response of the liquid crystals is less than 0.2 seconds.

C. DESCRIPTION OF LIQUID CRYSTAL SHEETS

Mylar sheeting was chosen for the foundation of the liquid crystal, because it is thin, pliable and has a small thermal conductivity, which for this system results in negligible heat transfer along the sheet.

The mylar sheet was cut into a 7 15/16" square with a 4 1/8"x 1/2" notch cut into the sheet for the experimental runs (Figure 7). The liquid crystals were applied to the mylar sheets with a Paasche, Model H "3 in 1" air brush. The steps taken in preparing the liquid crystal sheets were:

A. Thoroughly clean both sides of mylar sheet with acetone.

B. Use liquid slurry received from NCR without dilution.

C. Spray first coat of liquid crystals on one side of the clean mylar surface allowing the crystal to dry for 40 to 60 minutes.

D. Spray second coat and allow to dry for 20 minutes.

E. Spray third coat and allow to dry for one hour.

F. Apply the first coat of Testor's flat black paint on the dryed liquid crystals and allow to dry for 30 minutes.

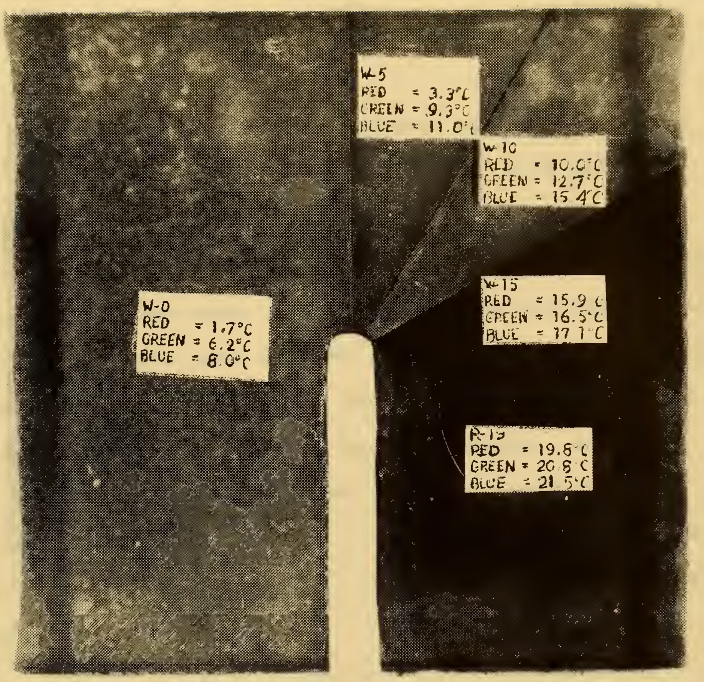

LIQUID CRYSTALS SPRAYED ON A MYLAR SHEET, THE SHEET IS ENCASED IN THE LIQUID CRYSTAL FRAME.

FIGURE 7

[illegible]

[illegible]

G. Apply the second coat and let dry for one hour.

H. Apply two coats of Rex Polyurethane Interior-Exterior 77-5 over the black paint paying particular attention to the edges. This will water proof the liquid crystal sheet.

The mylar sheet for the experimental run was divided into five areas (Figure 8). The W-5, W-10, R-15 and R-19 areas were covered with masking tape. W-0 crystals were applied as described earlier, but only one coat of Testor's flat black paint was used. The W-5 area was uncovered next and the W-5 crystals were sprayed. Then one coat of Testor's flat black paint was applied to the W-5 area. The process was repeated for the W-10, R-15 and R-19 areas. A second coat of Testor's flat black paint was then applied to the entire sheet and allowed to dry. The sheet was then water proofed. The reader is referred to Appendix A for calibration technique and data.

D. TEST CELL

The test cell was composed of two parts. The first was the liquid crystal sheet frame. The frame, which supported the liquid crystal sheet, was 7 15/16 inches square and was made up of two plexiglass squares that were screwed together with the liquid crystal sheet in the middle (Figure 8). On one side of the frame was a 0.5 inch diameter hole through which the cryoprobe fit.

The second part was a clear plexiglass 8 inch cube. Four inches down from the top of the cube was a 0.5 inch

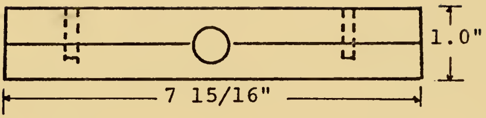

SIDE VIEW

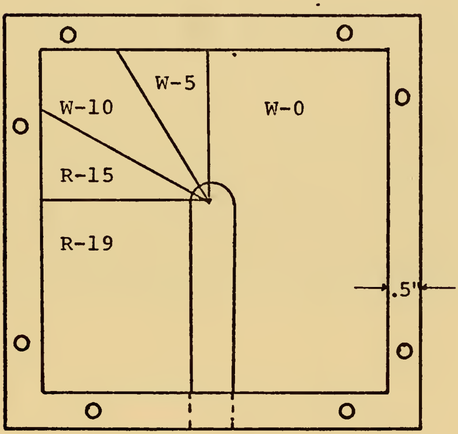

TOP VIEW

LIQUID CRYSTAL FRAME WITH
LIQUID CRYSTAL SHEET

FIGURE 8

wide shelf that supported the liquid crystal frame (Figure 9). A 0.5 inch diameter hole in the side of the box corresponded to the hole in the frame. When the cryoprobe was placed through the hole in the box and the frame, the longitudinal axis of the cryoprobe was in the same plane as the liquid crystal sheet.

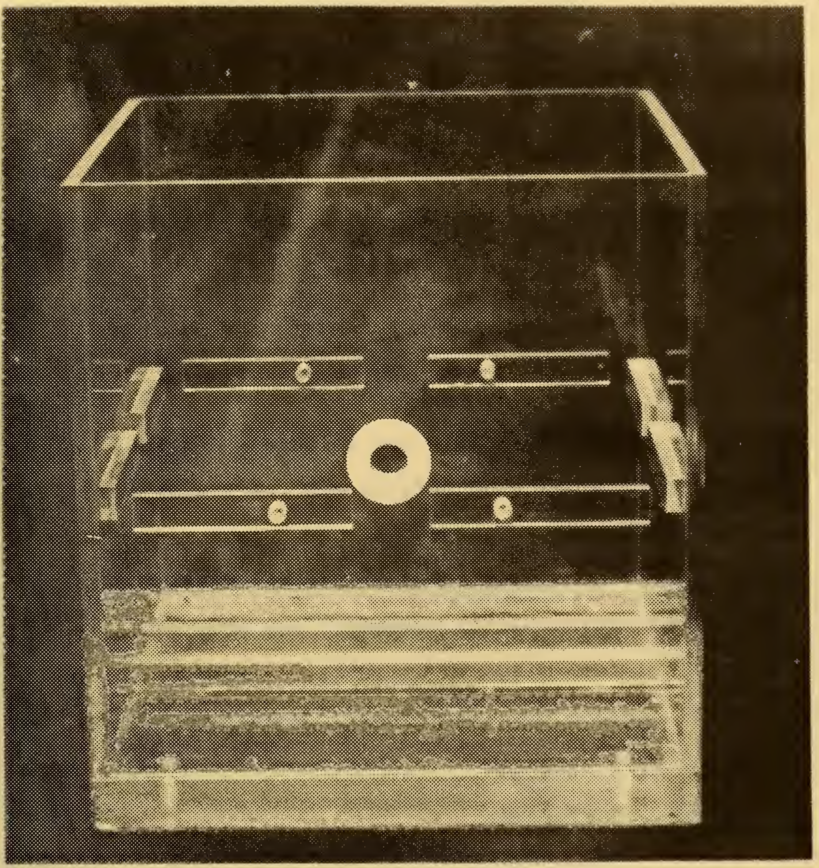

EIGHT INCH CUBICAL TEST CELL

FIGURE 9

[illegible]

IV. EXPERIMENTAL PROCEDURE

The liquid crystal frame was placed in the box. The cryoprobe was pushed through the hole in the box and the frame. A copper/constantan thermocouple was welded on the tip of the cryoprobe. To record the temperatures, a Honeywell Electronik 194 dual strip recorder with ice junction was used.

The gelatin was made and allowed to cool for six hours (Appendix C). After six hours the gelatin was cool enough to pour into the assembled box without thermally shocking the liquid crystals. The gelatin then was allowed to come to room temperature. The LN_2 dewar was connected to the cryoprobe by means of an insulated double wall tube (Figure 6). A vacuum pump was connected to the cryoprobe and the double wall tubing. A pressure of approximately 10mm of mercury was maintained in both probe and tubing. The Graflex camera (Appendix B) was positioned directly over the cryoprobe and all necessary adjustments were made. The thermocouples were connected to the strip recorder. The pressure on the LN_2 dewar was between 3 and 9.5 psi.

At time equal zero the LN_2 was turned on. The tip temperature was monitored with the recorder. When the tip temperature reached a predetermined temperature, the controls on the dewar were adjusted so the tip temperature remained constant. Pictures were taken at times of 0, 1, 3, 5, 10, 15, 30 and every 15 minutes thereafter until the 21.5°C

isotherm moved to the edge of the box. At this point in time the experiment was terminated.

The photographs recorded the isotherms and ice ball diameter. Using photo interpolation (knowing the probe diameter to be 0.50 inches) the actual ice ball diameter and the distance from the cryoprobe tip center to the various isotherms were determined.

Six experimental runs were made varying the probe tip temperatures as shown below:

Experiment	Tip Temperature	Initial Gelatin Temperature
1.	-36°C	22°C
2.	-53°C	21°C
3.	-65°C	21°C
4.	-75°C	20°C
5.	-97°C	25.5°C
6.	-117°C	22.5°C

In all cases the phase change temperature was -2.0°C. This was found by allowing the strip chart recorder to run for one hour after the experiment ended. The probe tip thermocouple steadied on -2°C and remained there until the ice ball had completely melted away from the cryoprobe.

Figure 10 shows a segment of chart paper for a typical experimental run. The first half is the response when the LN_2 is turned on and the second half is the response when the LN_2 is turned off.

Figures 11, 12, 13, and 14 show the ice ball forming in the gelatin with the liquid crystals visually presenting

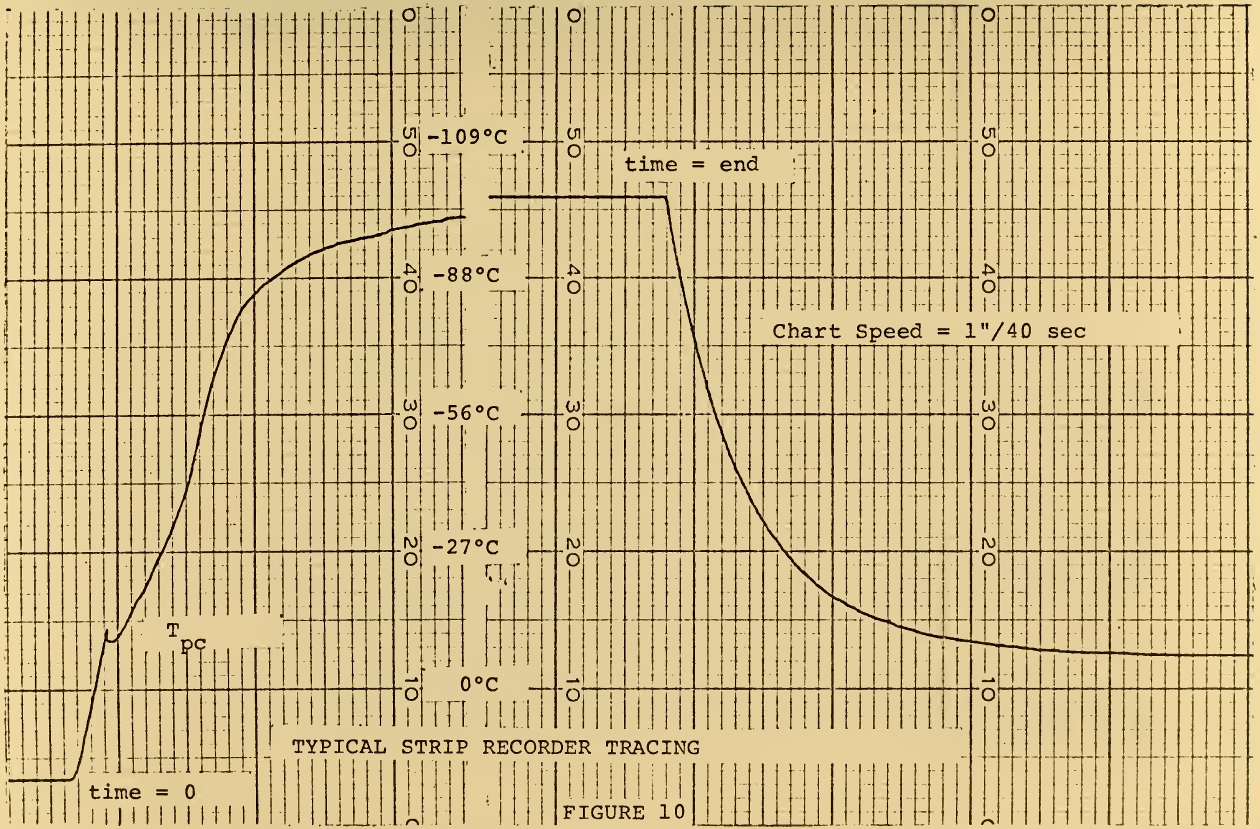

TYPICAL STRIP RECORDER TRACING

FIGURE 10

the isotherms. The relationship between the colors and temperatures are:

	Red	Green	Blue
W-0	1.7°C	6.2°C	8.0°C
W-5	3.3°C	9.3°C	11.0°C
W-10	10.0°C	12.7°C	15.4°C
R-15	15.9°C	16.5°C	17.1°C
R-19	19.8°C	20.8°C	21.5°C

0.5 INCH CRYOPROBE EMBEDDED IN THE GELATIN SURROUNDED BY THE LIQUID CRYSTAL SHEET AT TIME EQUAL ZERO. SEE FIGURE 7 FOR COLOR TEMPERATURE RELATIONSHIPS.

FIGURE 11

0.5 INCH CRYOPROBE EMBEDDED IN THE GELATIN SURROUNDED BY THE LIQUID CRYSTAL SHEET AT TIME EQUAL FIVE MINUTES. SEE FIGURE 7 FOR COLOR TEMPERATURE RELATIONSHIPS.

FIGURE 12

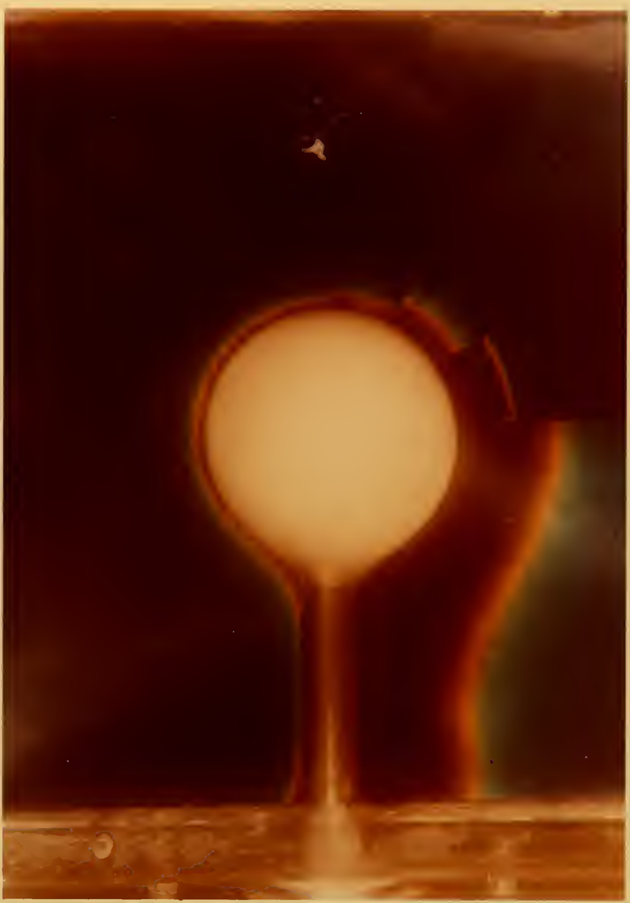

0.5 INCH CRYOPROBE EMBEDDED IN THE GELATIN
SURROUNDED BY THE LIQUID CRYSTAL
SHEET AT TIME EQUAL THIRTY MINUTES
SEE FIGURE 7 FOR COLOR TEMPERATURE RELATIONSHIPS.

FIGURE 13

0.5 INCH CRYOPROBE EMBEDDED IN THE GELATIN SURROUNDED BY THE LIQUID CRYSTAL SHEET AT TIME EQUAL SIXTY MINUTES. SEE FIGURE 7 FOR COLOR TEMPERATURE RELATIONSHIPS.

FIGURE 14

V. THEORETICAL ANALYSIS

When a cryoprobe is inserted into tissue and brought to a cryogenic temperature, a thermal field develops in the tissue. A lesion is formed as the tissue in the immediate vicinity of the cryoprobe undergoes a phase change. The freezing front will propagate through the tissue until steady state is reached within the tissue. The specific heat, density, thermal conductivity and latent heat of fusion, as well as blood flow and metabolism all contribute in controlling ultimate lesion size and growth rate for a given cryoprobe diameter and particular tip temperature. Therefore, to predict lesion size in a structure such as a human brain, it is necessary to know not only the cryoprobe tip temperature, but also the thermal properties of the structure immediately adjacent to the cryoprobe tip [4].

There have been several models [1, 6, 7] that describe the transient behavior of a cryolesion. Cooper and Trezek [6, 7] present an approximate solution to the problem of transient freezing around cylinders and spheres embedded in tissue. Their model included terms for the thermal properties, as well as for blood flow and metabolism. While the blood flow and metabolism terms are important, they have been disregarded in this study. In order to take the phenomenon into account, a live brain is necessary. Since the school lacked the proper facilities for operating on experimental animals, it was decided to experimentally

investigate the rate of ice formation produced by a cryoprobe embedded in gelatin. The experimental results were compared to the analytical solution of Cooper and Trezek to ascertain if their basic premise (neglecting heat capacity effects in both the frozen and unfrozen phases) is valid.

The following is a brief development of the solution presented by Cooper and Trezek without metabolism and blood flow terms.

The energy equation (see Nomenclature for definition of terms)

$$\rho c \frac{\partial T}{\partial t} = k\nabla^2 T \qquad (1)$$

is used to describe the temperature field around the cryoprobe. The energy equation will take the following form when used to describe one dimensional heat transfer in the frozen and unfrozen regions surrounding a spherical probe.

Unfrozen region

$$\rho c \frac{\partial T}{\partial t} = k\nabla^2 T = \frac{k}{r^2} \frac{\partial}{\partial r} \left(r^2 \frac{\partial T}{\partial r} \right) \qquad (2)$$

Frozen region

$$\rho c_f \frac{\partial T}{\partial t} = k_f \nabla^2 T_f = \frac{k_f}{r^2} \frac{\partial}{\partial r} \left(r^2 \frac{\partial T_f}{\partial r} \right) \qquad (3)$$

with the following boundary conditions

$$r = r_o \qquad T_f = T_s \qquad (4)$$

$$r = \qquad T_f = T_{pc} = T \qquad (5)$$

$$r \rightarrow \infty \qquad T = T_o \qquad (6)$$

$$r = \qquad k_f \frac{\partial T_f}{\partial r} = k \frac{\partial T}{\partial r} + \rho L \frac{\partial \mathcal{R}}{\partial t} \qquad (7)$$

By introducing the following non-dimensional groups,

$$\theta_f = \frac{T_f - T_o}{T_s - T_o} \qquad \theta = \frac{T - T_o}{T_s - T_o} \qquad \theta_{pc} = \frac{T_{pc} - T_o}{T_s - T_o}$$

$$R = \frac{r}{r_o} \qquad r^* = \frac{\ell}{r_o} \qquad \tau = \frac{k(T_o - T_{pc})t}{\rho L r_o{}^2}$$

the normalized energy equation becomes:

frozen region

$$\frac{1}{R^2} \frac{\partial}{\partial R} \left(R^2 \frac{\partial \theta_f}{\partial R} \right) = \frac{k\, c_f\, (T_o - T_{pc})}{k_f\, L} \frac{\partial \theta_f}{\partial \tau} \tag{8}$$

unfrozen region

$$\frac{1}{R^2} \frac{\partial}{\partial R} \left(R^2 \frac{\partial \theta}{\partial R} \right) = \frac{c\, (T_o - T_{pc})}{L} \frac{\partial \theta}{\partial \tau} \tag{9}$$

with the boundary conditions 4, 5, 6, and 7 becoming

$$R = 1 \qquad \theta_f = 1 \tag{10}$$

$$R = r^* \qquad \theta_f = \theta_{pc} = \theta \tag{11}$$

$$R \rightarrow \infty \qquad \theta \rightarrow 0 \tag{12}$$

$$R = r^* \qquad k_f \frac{\partial \theta_f}{\partial R} = k \frac{\partial \theta}{\partial R} - k\theta_{pc} \frac{\partial r^*}{\partial \tau} \tag{13}$$

Analytical solutions of equation (8) and (9) satisfying conditions (10), (11), (12), and (13) are not known. However, if we assume $\frac{k\, c_f (T_o - T_{pc})}{k_f L}$ and $\frac{c\, (T_o - T_{pc})}{L}$ are small, that is, if the heat capacity effects are small compared to latent heat effects (8) and (9) take the approximate form:

frozen region

$$\frac{1}{R^2} \frac{\partial}{\partial R} \left(R^2 \frac{\partial \theta_f}{\partial R} \right) = 0 \tag{14}$$

unfrozen region

$$\frac{1}{R^2} \quad \frac{\partial}{\partial R} \left(R^2 \frac{\partial \theta}{\partial R} \right) = 0 \qquad (15)$$

the solutions to equations (14) and (15) are

unfrozen region

$$\theta = \frac{\theta_{pc}\ r^*}{R} \qquad (16)$$

frozen region

$$\theta_f = 1 + \left(\frac{r^*}{r^*-1} \right) \left(1 - \theta_{pc} \right) \left(\frac{1}{R} - 1 \right) \qquad (17)$$

Equations (18) and (19) are substituted into equation (13) to find

$$\frac{dr^*}{d\tau} = \left(\frac{k_f}{k} \right) \left(\frac{1}{\theta_{pc}} \right) \left(\frac{1 - \theta_{pc}}{r + (r^*-1)} \right) - \frac{1}{r^*} \qquad (18)$$

Further rearrangement of equation (18) yields

$$d\tau = \frac{r^*\ (1 - r^*)}{(r^* + \eta)} \quad dr^* \qquad (19)$$

where

$$\eta = \frac{k_f}{k} \left(\frac{\theta_{pc} - 1}{\theta_{pc}} \right) - 1$$

at steady state $\frac{dr^*}{d\tau} = 0$, this necessitates from equation (19) that

$$r^* = -\eta \qquad (20)$$

at steady state. Integrating (19) between the limits 1 and $-\eta$ yields:

$$\tau = (\eta+1)\ (r^*-1) + \eta(\eta+1) \ln \frac{\eta+1}{\eta+r^*} - \frac{1}{2}\ (r^*-1) \qquad (21)$$

Using equation (20) and (21) an analytical prediction of the rate of growth of the ice ball can be made. A

FORTRAN program (Appendix E) was written that uses equation (20) and (21) to predict the rate of lesion growth. The program also predicts time to steady state and maximum lesion size for the particular cryoprobe size and tip temperature.

When using the FORTRAN program written in conjunction with this thesis the actual radius of the hemispherical cryoprobe tip is used vice a modified radius. At the beginning of this study it was felt that perhaps the radius should be the radius of an imaginary sphere that has the same surface area as the hemispherical cryoprobe tip since the theoretical analysis assumed a spherical case. However, the best agreement between the theoretical solution and experimental data occurred when the actual hemispherical radius of the cryoprobe tip was used in the FORTRAN program.

VI. RESULTS

Correlation between the experimental data and the theory was excellent. The theoretical curves for the six different cryoprobe tip temperatures, as calculated by the FORTRAN program (Appendix E), are illustrated in Figures 15, 16, 17, 18, 19, and 20. The experimental data is superimposed on the graphs to demonstrate the agreement. For the first hour the correlation is almost exact, then the experimental data starts to rise above the theoretical curve, but remains within the uncertainty bounds (Appendix D). The rise in the experimental data can be explained by the theoretical boundary conditions not being met after the first hour. That is, the 19°C isotherm had moved to the edge of the test cell and the gelatin no longer qualified as an "infinite" medium.

Figure 21 is a typical graph of the nondimensional time vs. nondimensional radius for a tip temperature of -25°C. The solid line represents the theoretical solution and the dashed lines represent the uncertainty bounds. The reader is referred to Appendix D for details on the uncertainty analysis.

The transient temperature field shows the details of a lesion formation. An example is illustrated in Figure 22. The discontinuity at -2°C, the phase change temperature, indicates the lesion size at a particular time after initiating cooling. The experimental points on the graph were

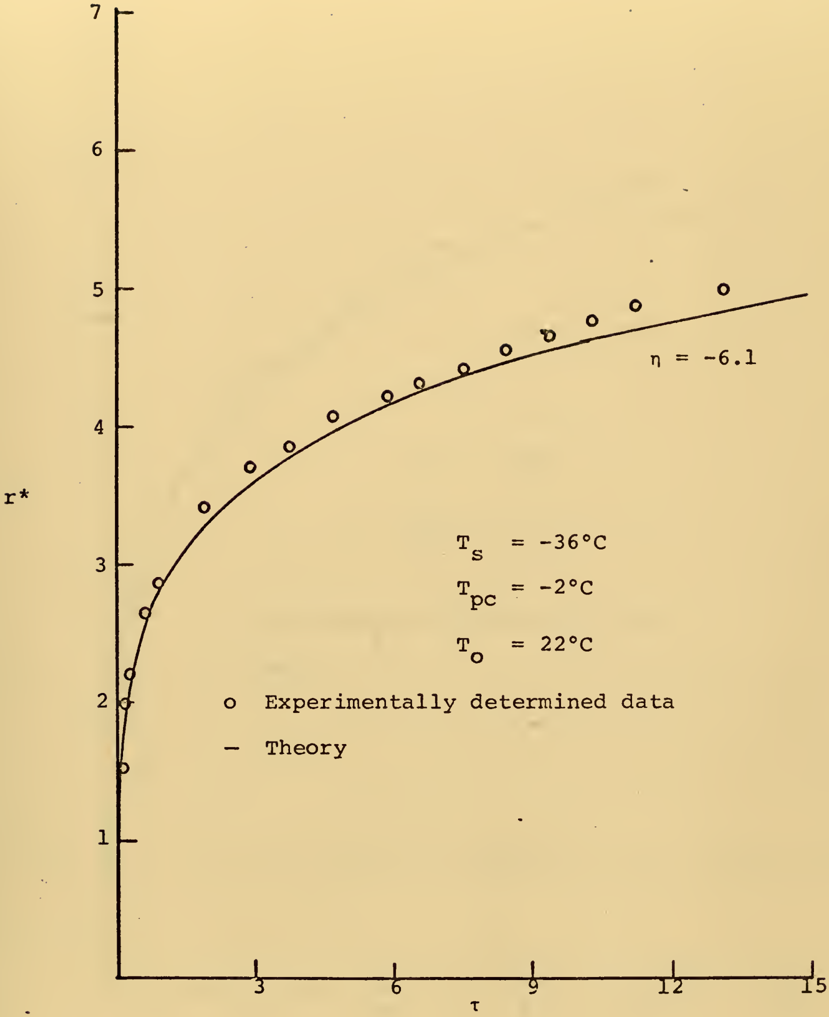

COMPARISON OF THEORETICAL AND EXPERIMENTAL PREDICTION OF ICE FRONT LOCATION, r*, AS A FUNCTION OF TIME, τ, FOR A PROBE TEMPERATURE OF -36°C.

FIGURE 15

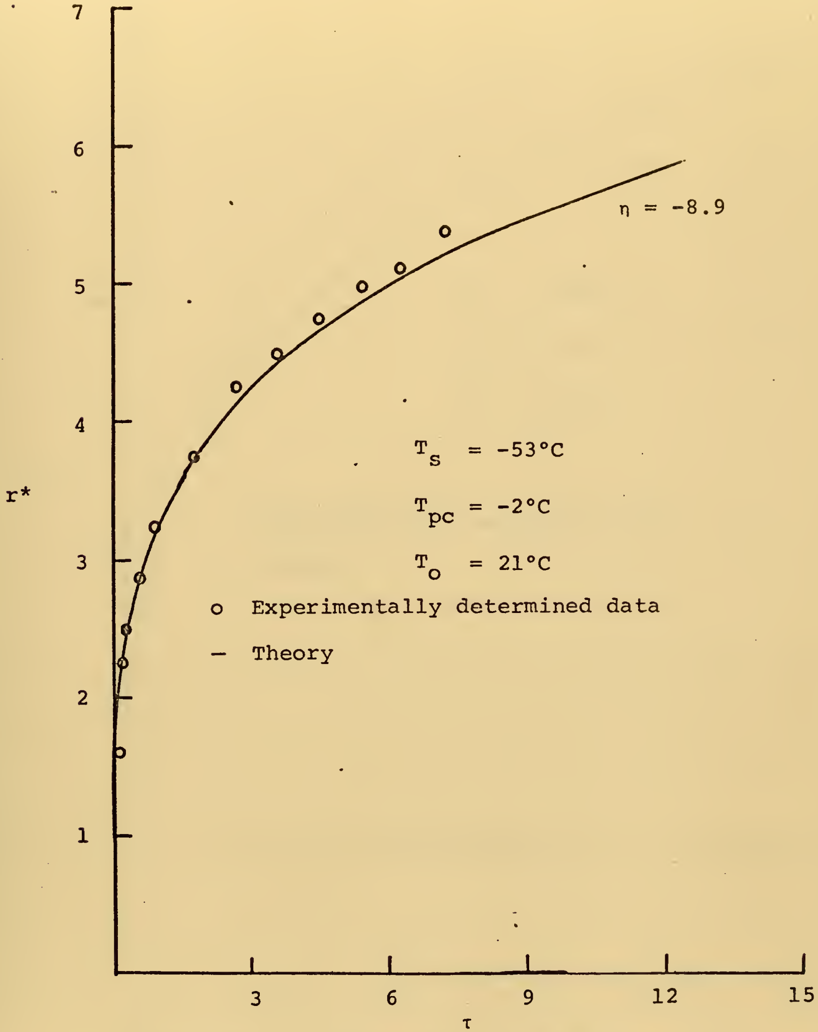

COMPARISON OF THEORETICAL AND EXPERIMENTAL PREDICTION OF ICE FRONT LOCATION, r*, AS A FUNCTION OF TIME, τ, FOR A PROBE TEMPERATURE OF -53°C.

FIGURE 16

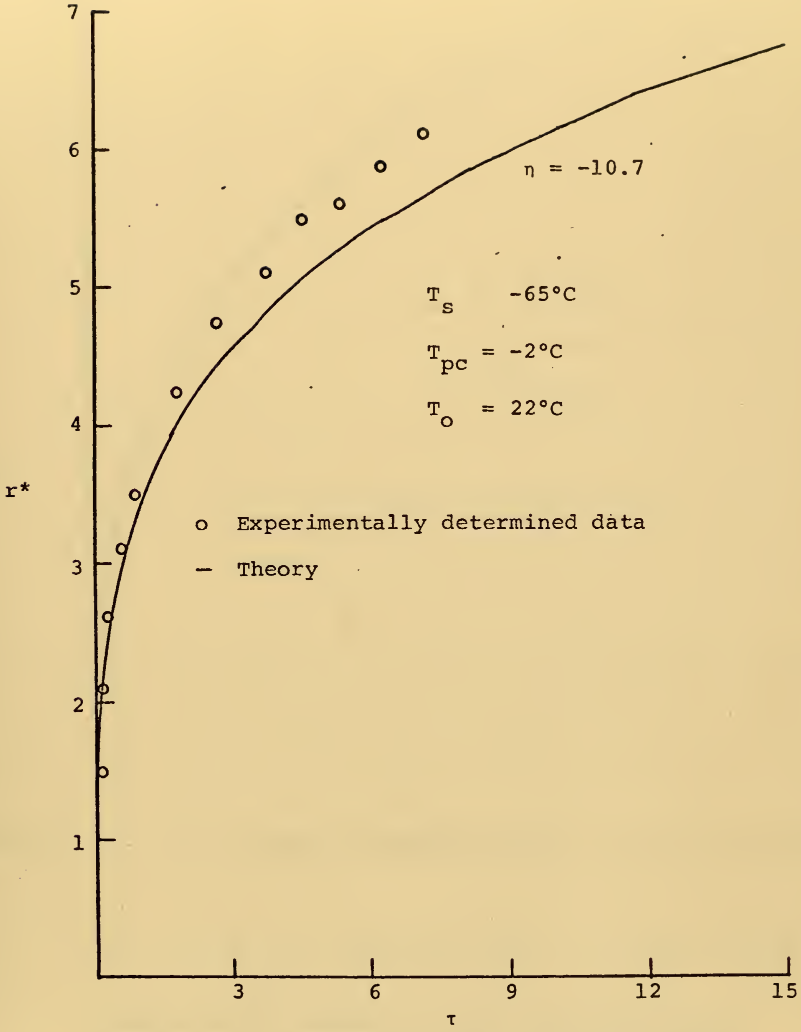

COMPARISON OF THEORETICAL AND EXPERIMENTAL PREDICTION OF ICE FRONT LOCATION, r*, AS A FUNCTION OF TIME, τ, FOR A PROBE TEMPERATURE OF -65°C.

FIGURE 17

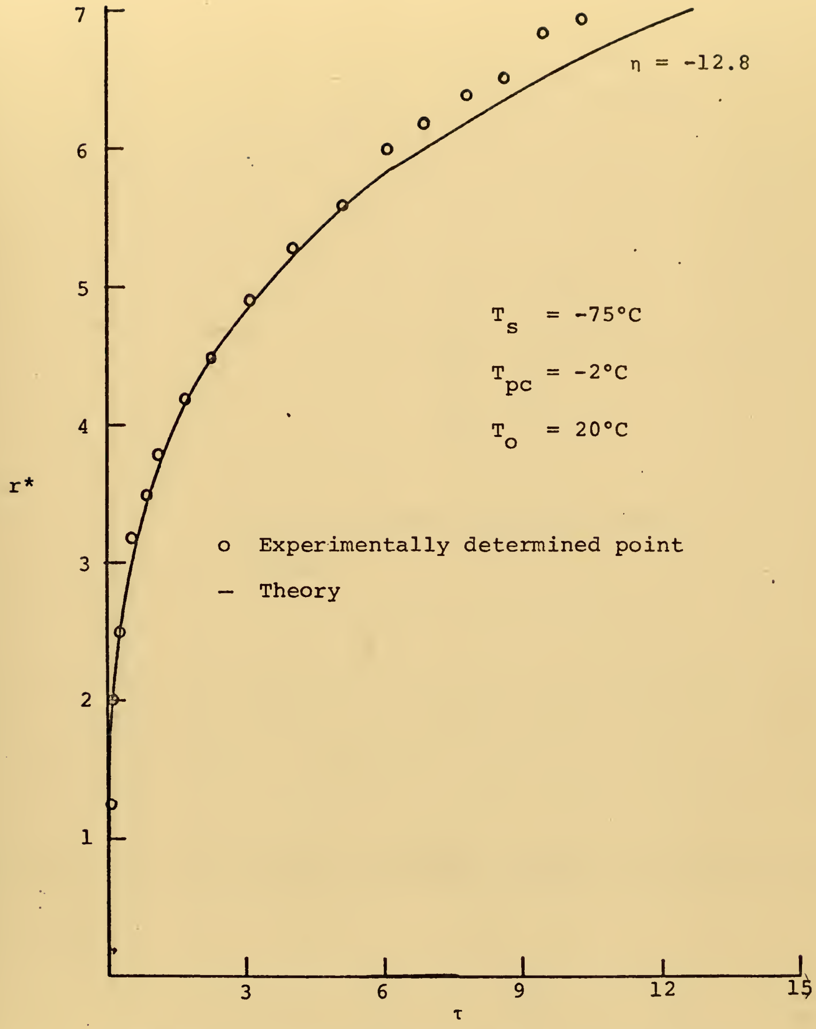

COMPARISON OF THEORETICAL AND EXPERIMENTAL PREDICTION OF ICE FRONT LOCATION, r*, AS A FUNCTION OF TIME, τ, FOR A PROBE TEMPERATURE OF -75°C.

FIGURE 18

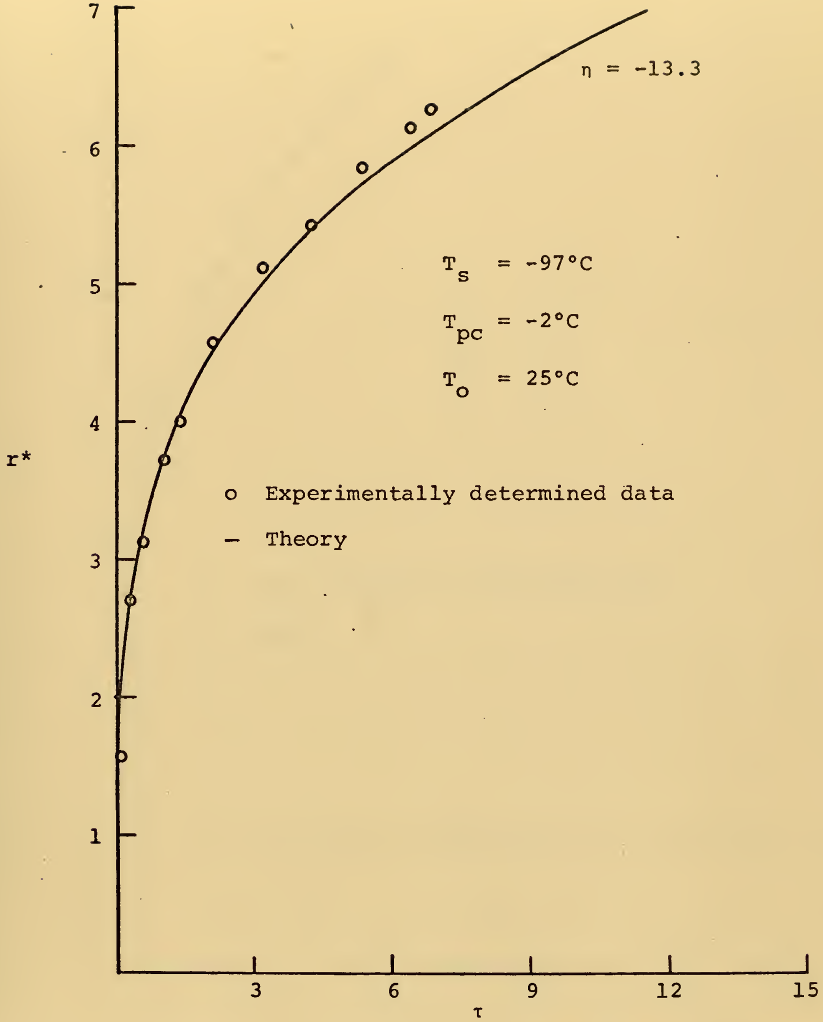

COMPARISON OF THEORETICAL AND EXPERIMENTAL PREDICTION OF ICE FRONT LOCATION, r*, AS A FUNCTION OF TIME, τ, FOR A PROBE TEMPERATURE OF -97°C.

FIGURE 19

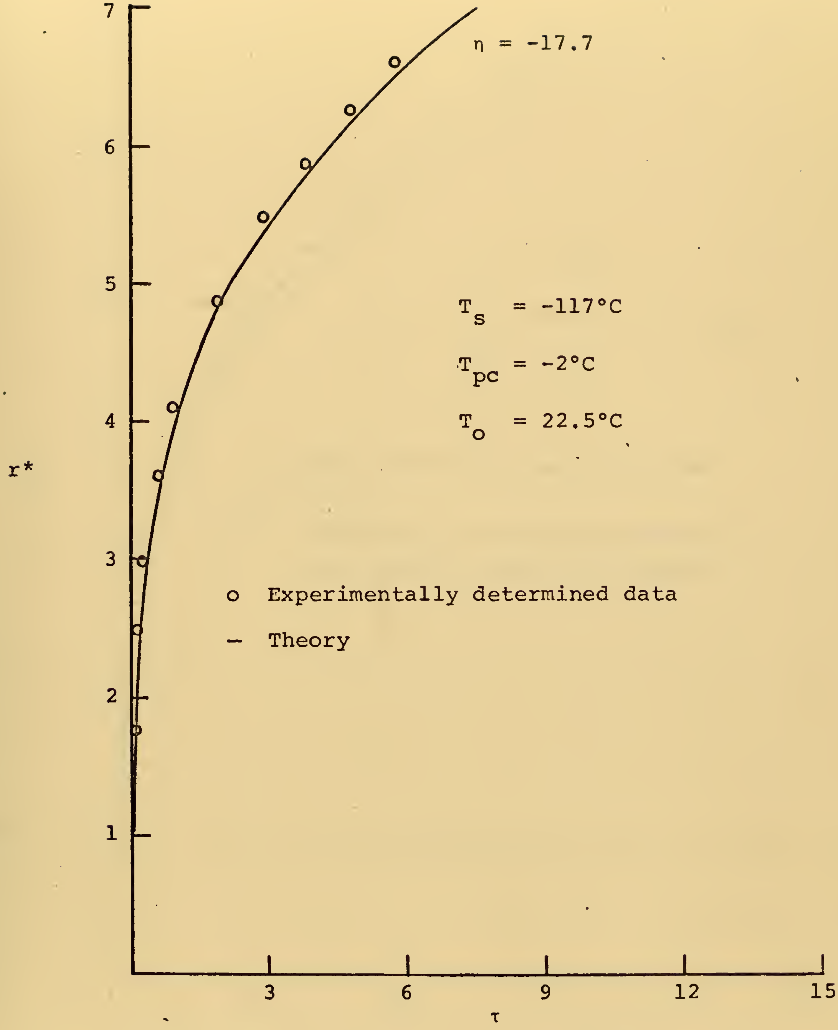

COMPARISON OF THEORETICAL AND EXPERIMENTAL PREDICTION OF ICE FRONT LOCATION, r^*, AS A FUNCTION OF TIME, τ, FOR A PROBE TEMPERATURE OF -177°C.

FIGURE 20

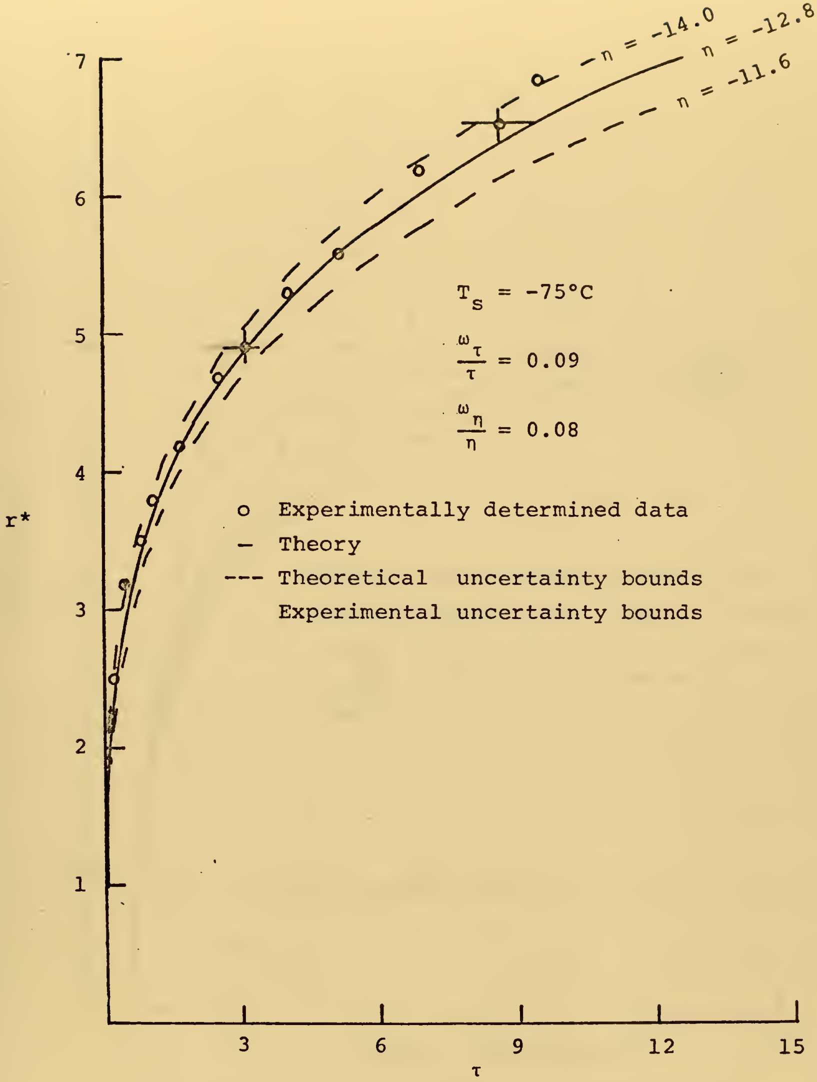

GRAPH OF THE UNCERTAINTY BOUNDS OF THE THEORETICAL CURVE AND UNCERTAINTY LIMITS OF THE EXPERIMENTALLY DETERMINED DATA AT A CRYOPROBE TIP TEMPERATURE OF -75°C.

FIGURE 21

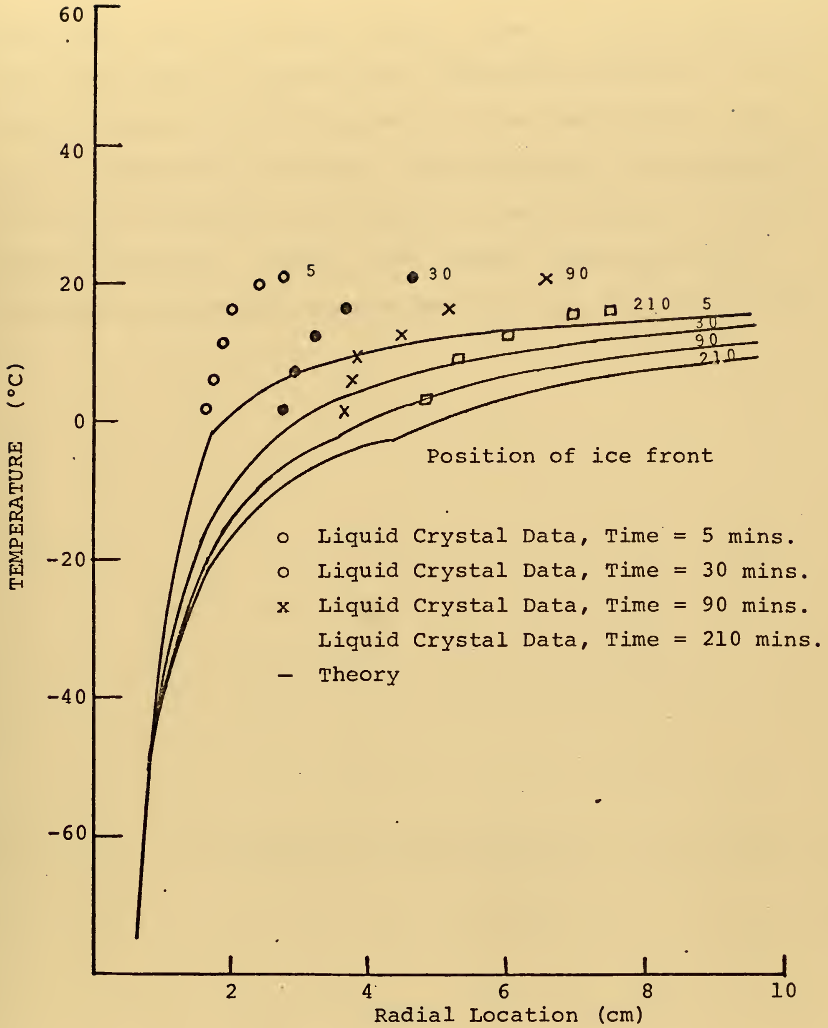

GRAPH OF THE TRANSIENT TEMPERATURE FIELD AT TIMES OF 5, 30, 90, 210 MINUTES AT A CRYOPROBE TIP TEMPERATURE OF -75°C.

FIGURE 22

determined from the liquid crystal sheet. The experimentally determined points show that the temperature gradient in the unfrozen phase is much sharper than the theoretically predicted temperature gradient. This difference is attributed to the heat capacity effect which is neglected in the theoretical analysis. However, the thermal capacitance does not seem to be important in determining the ice growth rate.

VII. CONCLUSIONS AND RECOMMENDATIONS

The use of liquid crystals afforded an unique opportunity to visually witness the rate of movement of various isotherms. The analytical prediction of the lesion growth rate, as presented by Cooper and Trezek, shows good agreement with experimentally determined data. The assumption made in the theoretical analysis, that the heat capacity in the frozen phase is negligible, seems reasonable. However, the thermal capacity in the unfrozen region does have a definite influence on the extent of the temperature field.

The ability to control the tip temperature was difficult at higher temperatures (-36°C, -53°C) and relatively easy at lower temperatures (-117°C). It is recommended that an automatic control system be developed to control the cryoprobe tip temperature.

The smaller cryoprobe should function properly if the tip were redesigned so as to be hemispherical. Also when the small cryoprobe is used in an experimental run, low LN_2 pressure (1.5 to 3.5 psig) should be used.

APPENDIX A

Liquid Crystals

For this project seven different temperature ranges of the cholesteric type were used. The manufacturer was National Cash Register (NCR). The crystals used were: (NCR Notation)

A. W-0

B. W-5

C. W-10

D. R-15

E. R-19

F. R-23

G. R-27

W - wide temperature range -5°C

R - regular temperature range 4°C

No information was received as to the exact temperature at which color changes would occur nor the exact meaning of the ranges 5°/4°C. Thus it was necessary to calibrate the crystals prior to any experimentation to find their ranges of utilization.

Two calibration mylar sheets were prepared. Both sheets were four inch square. The same technique used for preparing the liquid crystal sheet used in the experiment was used for preparing the calibration sheets. Each sheet was divided into fourths. The first sheet contained the W-0, W-5,

W-10, and R-15 crystals. The second sheet was similarly divided with R-19, R-23, and R-27 applied. Each sheet was calibrated separately in the Rosemount, model 913A, calibration bath (constant temperature bath). The bath was lowered to 0°C. The first sheet, containing W-0, W-5, W-10 and R-15, was placed in the bath. The bath temperature was monitored by a Rosemount Commutating Bridge, model 92A, and galvanometer arrangement with a Rosemount Platinum Resistance Temperature Standard 162C. Throughout the calibration procedure one observer read the color changes while the other read the commutating Bridge. The following results were obtained.

Calibration of Liquid Crystals

	Red	Green	Blue
W-0	1.7°C	6.2°C	8.0°C
W-5	3.3°C	9.3°C	11.0°C
W-10	10.0°C	12.7°C	15.4°C
R-15	15.9°C	16.5°C	17.1°C
R-19	19.8°C	20.8°C	21.5°C
R-23	22.4°C	23.5°C	24.6°C
R-27	26.7°C	27.9°C	28.9°C

APPENDIX B

Photographic Techniques

In order to make a permanent record of the experiments, pictures were required. For data taking Polaroid Polacolor 4 x 5 land film Packets, color/type 58, were used in a Graflex camera (4 x 5 press Graflex). The experimental runs were made at night. The lighting was supplied by a Tungsten 3200°K light. The film used was a daylight type necessitating the use of a Tiffen Photar Filter 80B series 6 for color. When taking pictures for publication quality, 35mm high speed Ektachrome color film was used in a Honeywell Pentax H-3. This film was designed for use with the Tungsten 3200°K lights.

In both cases the technique used for taking the pictures was the same. The camera, on a tripod, was placed directly over the cryoprobe. The camera was focused and settings were made. The Tungsten light was placed approximately six feet away from the cryoprobe. When a picture was desired, the Tungsten 3200°K light was turned on, the room lights turned off and the picture taken. As soon as the picture was taken, the Tungsten light was turned off. The total time the Tungsten light was left on was approximately ten seconds. It was felt that the heat generated by the light had little or no effect on the freezing rate.

The general photographic techniques were used when taking pictures through the gelatin. The highest f stop

with the slowest shutter speed was used to get the greatest depth of field. The main drawback with the Polaroid film was that it was a daylight film with a reasonable ASA, but when the filter was added the ASA was lowered to 24. Color reproduction was considered adequate for data taking.

APPENDIX C

Preparing the Gelatin

To make the gelatin the following recipe was used:

a. Heat 6800 ml of water to boiling
b. Soak 120 gms of Schilling's Gelatin in 1200 ml of cold water for 3 minutes. Do not disturb during this time.
c. Pour boiling water into the gelatin mixture.
d. Stir gently while pouring in the hot water. If stirred too vigorously a foam will appear on the surface.
e. After all hot water is in gelatin mixture, stir to insure all gelatin is thoroughly mixed.
f. Leave gelatin in mixing container and put in refrigerator (initial temperature 32°F) for 3 hours.
g. Take out of refrigerator and let stand at room temperature for 3 hours.
h. Pour into experimental box.
i. Let stand at room temperature for 12 hours. Gelatin is now ready for use.

APPENDIX D

The uncertainty in a function f(x,y,z) computed from measured values of several independent quantities (x,y,z) may be estimated as

$$\frac{\omega_f}{f} = \sqrt{\left(\frac{\partial f}{\partial x}\,\frac{\omega_x}{f}\right)^2 + \left(\frac{\partial f}{\partial y}\,\frac{\omega_y}{f}\right)^2 + \left(\frac{\partial f}{\partial z}\,\frac{\omega_z}{f}\right)^2} \qquad (1)$$

where ω_f is the estimated uncertainty in f due to estimated uncertainties of ω_x, ω_y, ω_z in x, y, z respectively [2, 11].

Such an uncertainty analysis was carried out on the quantities $\eta = \frac{k_f}{k}\left(\frac{T_{pc} - T_s}{T_{pc} - T_o}\right) - 1$ and $\tau = \frac{k(T_o - T_{pc})\,t}{\rho L r_o^2}$ to ascertain the influence of experimental uncertainties on the theoretical and experimental determinations of r*. Applying (1) to η and τ it is found:

$$\frac{\omega_\eta}{\eta} = \sqrt{\left(\frac{\omega_{k_f}}{k_f}\right)^2 + \left(\frac{\omega_k}{k}\right)^2 + \left(\frac{\omega_{T_{pc} - T_s}}{T_{pc} - T_s}\right)^2 + \left(\frac{\omega_{T_{pc} - T_o}}{T_{pc} - T_o}\right)^2}$$

and

$$\frac{\omega_\tau}{\tau} = \sqrt{\left(\frac{\omega_k}{k}\right)^2 + \left(\frac{\omega_{T_o - T_{pc}}}{T_o - T_{pc}}\right)^2 + \left(\frac{\omega_t}{\tau}\right)^2 + \left(\frac{\omega_\rho}{\rho}\right)^2 + \left(\frac{\omega_L}{L}\right)^2 + \left(\frac{2\omega_{r_o}}{r_o}\right)^2}$$

The following are the estimated true values and uncertainties for the experimental run with the probe temperature held at -75°C.

$T_{pc} - T_s = -77°C \pm 1°C$ 20:1

$T_{pc} - T_o = -22°C \pm 1°C$ 20:1

$$k = 0.0014 \pm .0001 \frac{\text{Cal}}{{}^{\circ}\text{C cm sec}} \qquad 20:1$$

$$k_f = 0.0050 \pm .0001 \frac{\text{Cal}}{{}^{\circ}\text{C cm sec}} \qquad 20:1$$

$$\rho = 1.00 \pm .01 \frac{\text{gm}}{\text{Cm}^3} \qquad 20:1$$

$$L = 79.71 \pm .01 \frac{\text{Cal}}{\text{gm}} \qquad 20:1$$

$$r_o = 0.025 \pm .002 \text{ Cm} \qquad 20:1$$

$$\frac{\omega_{T_{pc} - T_s}}{T_{pc} - T_s} = 0.01 \qquad \frac{\omega_\rho}{\rho} = 0.01$$

$$\frac{\omega_{T_{pc} - T_o}}{\omega_{T_{pc} - T_o}} = 0.05 \qquad \frac{\omega_L}{L} = 0.01$$

$$\frac{\omega_k}{k} = 0.07 \qquad \frac{\omega_{r_o}}{r_o} = 0.01$$

$$\frac{\omega_{k_f}}{k_f} = 0.02$$

The results of the uncertainty analysis indicated that for this particular run:

$$\frac{\omega_\tau}{\tau} = 0.09 \quad \text{and} \quad \frac{\omega_\eta}{\eta} = 0.09$$

Similar calculations were made on the other five experimental runs and in all cases $\frac{\omega_\tau}{\tau}$ and $\frac{\omega_\eta}{\eta}$ fell between 0.08 and 0.09. A typical uncertainty plot is shown in Figure 21.

APPENDIX E

```
        THIS PROGRAM WILL REDUCE EXPERIMENTALLY DETERMENED RADIUS OF THE
        ICE BALL AND THE ACTUAL TIME INTO RSTAR AND NONDIMENSIONAL TIME
        AND WILL PLOT THE THEORETICAL SOLUTION AS A CURVE AND WILL PLACE
        THE EXPERIMENTAL POINTS ALONG THE THEORETICAL CURVE

        IMPLICIT REAL*4(K)
        REAL*8 ITITLE(12)
        REAL LABLE
        DIMENSION TAU(50),RSTAR(50),TIME(50),EXPR(20),EXPT(20),EXPTA(20)
C       EXPR IS THE EXPEREMENTAL RSTAR
C       EXPT IS THE EXPEREMENTAL TIME
C       P IS THE DENSITY OF THE GEL
C       KF IS THE CONDUCTIVITY OF THE FROZEN REGION
C       K IS THE CONDUCTIVITY OF THE UNFROZEN REGION
C       PER IS THE RATIO OF RSTAR(REAL)/RSTAR(STEADY STATE)
C       TL IS THE LATENT HEAT
C       TAU IS THE NONDIMENSIONAL TIME
C       RSTAR IS THE NONDIMENSIONAL RADIUS
C       TO IS THE TEMPERATURE FAR FROM THE PROBE IN DEGREE CENT.
C       TS IS THE PROBE TIP TEMPERATURE IN DEGREE CENT.
C       TPC IS THE PHASE CHANGE TEMPERATURE IN DEGREE CENT.
C       RO IS THE PROBE RADIUS IN CM
C       NUNN IS THE TOTAL NUMDER OF EXPERIMENTAL DATA POINTS
        P=1.0
        KF=0.005
        K=0.0014
        RO=0.25
        RO=RO*2.54
        PER=0.95
        TL=79.71
        TS=-75.0
        TO=20.0
        TPC=-2.0
        NUNN=20
        THETA=(TPC-TS)/(TPC-TO)
        PHI=-(KF/K)*THETA
        CON=-(1.0+PHI)
        READ(5,3000)(ITITLE(L),L=1,10)
 3000   FORMAT(10A8)
        READ(5,4000)(ITITLE(L),L=11,12)
 4000   FORMAT(2A8)
C       EXPERMENTAL DATA INPUT
        READ(5,1700)(EXPR(I),I=1,11)
 1700   FORMAT(11F6.4)
        READ(5,1750)(EXPR(I),I=12,NUNN)
 1750   FORMAT(9F6.4)
        READ(5,1760)(EXPT(I),I=1,11)
 1760   FORMAT(11F6.4)
```

```
      READ(5,1770)(EXPT(I),I=12,NUNN)
 1770 FORMAT(9F6.4)
      DO 1900 I=1,NUNN
      EXPR(I)=(EXPR(I)*2.54)/(RO*2.0)
      EXPTA(I)=(K*(TO-TPC)*EXPT(I)*60.0)/(P*TL*RO**2)
 1900 CONTINUE
C     CALCULATING THE NUMBER OF NECESSARY TIME STEPS
 1000 TN=1.0-PER*((1.0+PHI)/PHI)+1.0/PHI
      TNUM=1.0/TN
      IF(TNUM.LT.50.0) GO TO 1100
      PER=PER-0.01
      GO TO 1000
 1100 NUM=TNUM-1.0
      TUM=1.0
      TUMY=NUM
C     CALCULATING RSTAR
 1200 DO 1300 I=1,NUM
      RSTAR(I)=1.0+(TUM/TNUM)*PHI
      TUM=TUM+1.0
      IF(TUM.GT.TUMY) GO TO 1400
 1300 CONTINUE
 1400 CON1=1.0+CON
      CON2=1.0+2.0*CON
C     CALCULATING THE REAL AND NONDIMENSIONAL TIME
      DO 1500 I=1,NUM
      AONE=RSTAR(I)-1.0
      BONE=RSTAR(I)+CON
      TAU(I)=CON2*AONE+CON*CON1*ALOG(CON1/BONE)+0.5*(CON1**2-BONE**2)
      TIME(I)=(TAU(I)*RO**2*TL*P)/(K*(TO-TPC))
      TIME(I)=TIME(I)/60.0
      A=TIME(I)
      IF(A.LT.290) GO TO 1950
      GO TO 1500
 1950 MOM=I
 1500 CONTINUE
      WRITE(6,2000)
 2000 FORMAT('1','EXPERMENTAL RSTAR',10X,'EXPERMENTAL TAU')
      WRITE(6,2025)
 2025 FORMAT('+',52X,'EXPERMENTAL TIME(MINUTES)'///)
      DO 2050 I=1,NUNN
      WRITE(6,2055)EXPR(I),EXPTA(I),EXPT(I)
 2055 FORMAT('0',9X,F8.3,18X,F8.3,18X,F9.3)
 2050 CONTINUE
      WRITE(6,1490)
 1490 FORMAT('1',10X,'RSTAR',15X'TAU',15X'TIME (MINITES)',///)
      DO 1550 I=1,NUM
      WRITE(6,1600)RSTAR(I),TAU(I),TIME(I)
 1600 FORMAT('0',10X,F8.3,9X,F8.3,9X,F9.3)
```

```
 1550 CONTINUE
C     NECESSARY INPUTS FOR DRAW
      NUM=MOM
      LAST=0
      MODCUR=1
      NUMPTS=NUM
      IGRID=1
      IHIGH=7
      IWIDE=5
      MODYAX=0
      MODXAX=0
      IYRIGH=0
      IXUP=0
      EXSCAL=3
      ITYPE=0
      YSCALE=1
      READ(5,500) LABLE
 500  FORMAT(A4)
      CALL DRAW(NUMPTS,TAU ,RSTAR,MODCUR,ITYPE,LABLE,ITITLE,EXSCAL
     1,YSCALE,IXUP,IYRIGH,MODXAX,MODYAX,IWIDE,IHIGH,IGRID,LAST)
C     NECESSARY INPUTS FOR DRAW
      LAST=0
      MODCUR=3
      NUMPTS=NUNN
      IGRID=1
      IHIGH=7
      IWIDE=5
      MODYAX=0
      MODXAX=0
      IYRIGH=0
      IXUP=0
      EXSCAL=3
      ITYPE=3
      YSCALE=1
      READ(5,1780) LABLE
 1780 FORMAT(A4)
      CALL DRAW(NUMPTS,EXPTA,EXPR,MODCUR,ITYPE,LABLE,ITITLE,EXSCAL
     1,YSCALE,IXUP,IYRIGH,MODXAX,MODYAX,IWIDE,IHIGH,IGRID,LAST)
      STOP
      END
```

BIBLIOGRAPHY

1. Barron, R. F., "Heat Transfer Problems in Cryosurgery," *J. Cryosurgery*, v. 1, p. 316-325, No. 4, December 1968.

2. Beckwith, T. G., Buck, N. L., *Mechanical Measurement*, p. 95-103, Addison-Wesley, 1969.

3. Cooper, I. S., Gionino, G. and Terry, R., "The Cryogenic Lesion," 2nd Int. Symp. Stereoencephalotomy, Copenhagen 1965 *Confin. neurol* 26: p. 161-177, 1965.

4. Cooper, I. S., "Cryobiology as Viewed by the Surgeon," *J. Cryobiology*, v. 1, No. 1, p. 44-45, 1964.

5. Cooper, T. E., and Trezek, G. J., "A Probe Technique for Determining the Thermal Conductivity of Tissue," *J. Heat Transfer*, p. 133-140, May 1972.

6. Cooper, T. E., and Trezek, G. J., "Analytical Prediction of the Temperature Field Emanating from a Cryogenic Surgical Cannula," *J. Cryobiology*, v. 7, p. 79-93, No. 2-3, 1970.

7. Cooper, T. E., and Trezek, G. J., "Rate of Lesion Growth around Spherical and Cylindrical Cryoprobes," *J. Cryobiology*, v. 7, p. 183-190, No. 4-6, 1971.

8. Cowley, C. W., "Cryobiology as Viewed by the Engineer," *J. Cryobiology*, v. 1, No. 1, p. 40-43, 1964.

9. Lawrence Radiation Laboratory Report UCRL-14754, Rev. II, *Trump: A Computer Program for Transient and Steady State Temperature Distributions in Multidimensional Systems*, by A. L. Edwards, 1969.

10. Erbayram, C., *A Computer Program for Solving Transient Heat Conduction Problems*, M.S. Thesis, Naval Postgraduate School, 1971.

11. Kline, S. J. and McClintock, F. A., "Describing Uncertainties in Single Sample Experiments," *Mechanical Engineer*, v. 75, p. 3, January 1953.

12. Fergason, J. L., "Liquid Crystals," *Scientific American*, v. 211, p. 77-85, August 1964.

13. Army Missile Command Report RS-TR-70-4, *Practical Applications of Liquid Crystals*, by C. M. Forman, 1970.

14. Groff, J. P., Design and Analysis of a Resistively Heated Surgical Probe, M. S. Thesis, Naval Postgraduate School, 1971.

15. Meyer, J. F., Mackenize, D. K., Wirzburger, A. H., Thermal Mapping of Surface Temperatures Using Cholesteric Liquid Crystals, ME. 3430 Laboratory Project, Naval Postgraduate School, 9 June 1972.

16. National Cash Register, Encapsulated Liquid Crystals p. 1-4, May 1971.

17. Von Leden, H., and Cahan, W., Cryogenics in Surgery, Medical Examination Publishing Co., Inc., Flushing, New York, 1971.

INITIAL DISTRIBUTION LIST

		No. Copies
1.	Defense Documentation Center Cameron Station Alexandria, Virginia 22314	2
2.	Library, Code 0212 Naval Postgraduate School Monterey, California 93940	2
3.	Mechanical Engineering Department Library, Code 59 Naval Postgraduate School Monterey, California 93940	1
4.	Assistant Professor T. E. Cooper, Code 59Cg Department of Mechanical Engineering Naval Postgraduate School Monterey, California 93940	3
5.	LCDR William K. Petrovic c/o Commanding Officer Norfolk Naval Shipyard Portsmouth, Virginia	1
6.	Professor Paul Pucci, Code 59 PC Department of Mechanical Engineering Naval Postgraduate School Monterey, California 93940	1
7.	Associate Professor George Trezek Department of Mechanical Engineering University of California Berkeley, California	1

UNCLASSIFIED
Security Classification

DOCUMENT CONTROL DATA - R & D

(Security classification of title, body of abstract and indexing annotation must be entered when the overall report is classified)

1. ORIGINATING ACTIVITY *(Corporate author)* Naval Postgradaute School Monterey, California 93940	2a. REPORT SECURITY CLASSIFICATION Unclassified 2b. GROUP

3. REPORT TITLE
An Experimental Investigation of the Temperature Field Produced by a Surgical Cryoprobe

4. DESCRIPTIVE NOTES *(Type of report and inclusive dates)*
Master's Thesis; December 1972

5. AUTHOR(S) *(First name, middle initial, last name)*
William K. Petrovic

6. REPORT DATE December 1972	7a. TOTAL NO. OF PAGES 65	7b. NO. OF REFS 17
8a. CONTRACT OR GRANT NO. b. PROJECT NO. c. d.	9a. ORIGINATOR'S REPORT NUMBER(S) 9b. OTHER REPORT NO(S) *(Any other numbers that may be assigned this report)*	

10. DISTRIBUTION STATEMENT
Approved for public release; distribution unlimited.

11. SUPPLEMENTARY NOTES	12. SPONSORING MILITARY ACTIVITY Naval Postgraduate School Monterey, California 93940

13. ABSTRACT

The temperature field produced by a cryosurgical probe embedded in a clear gelatin-water test medium has been experimentally investigated. The temperature field emanating from the cryoprobe was measured using a thin mylar sheet sprayed with liquid crystals, a temperature sensitive material. Probe tip temperatures varying from -36°C to -117°C were studied. The experimental results compared within approximately 9% of a one dimensional analytical solution for predicting ice growth rate.

14. KEY WORDS	LINK A		LINK B		LINK C	
	ROLE	WT	ROLE	WT	ROLE	WT
Cryoprobe						
Cryogenic Surgical Cannula						
Lesion Growth						
Liquid Crystals						
Heat Transfer						
Cryosurgery						

141685

Thesis
P4575 Petrovic
c.1 An experimental investigation of the temperature field produced by a surgical cryoprobe.